

Observing Earth Trojans with Gaia ?

prepared by: F. Mignard, P. Tanga, M. Todd
affiliation : OCA
reference: GAIA-C4-TN-OCA-FM-051-1
issue: 1
revision: 0
date: 2011-10-31
status: Issued

Abstract

This note discusses the possibility of observing Earth Trojans with Gaia. The goals are to show the peculiarities of the observations of these objects and present some statistical results, assuming small bodies of about 0.5 km in diameter scattered around the two equilibrium Sun-Earth Lagrangian points L4 and L5.

Document History

Issue	Revision	Date	Author	Comment
I	0	2011-10-31	FM	Issued to LiveLink
D	0	2011-10-31	FM	Comments and suggestions from PT and MT included
D	0	2011-10-26	FM	Start of the document

Contents

1 Introduction **6**

2 Observability with Gaia **6**

3 Simulation **8**

4 Results of the simulation **8**

4.1 Solar elongations 10

4.2 Phases 13

4.3 Transit velocity 15

4.4 Number of transits 20

5 Conclusions **23**

Acronyms

The following table has been generated from the on-line Gaia acronym list:

Acronym	Description
CCD	Charge-Coupled Device
DPAC	Data Processing and Analysis Consortium
ETA	Earth-Trojan Asteroid
MBA	Main-Belt Asteroid
NEA	Near-Earth Asteroid
NEO	Near-Earth Object

References

[SAG-FM-007], Mignard, F., 2001, *Detection of Near Earth Objects with Gaia*, SAG-FM-007, URL http://www.rssd.esa.int/llink/livelink/open/359123

[SAG-FM-009], Mignard, F., 2001, *Observation of main belt asteroids with Gaia*, SAG-FM-009, URL http://www.rssd.esa.int/llink/livelink/open/359133

[FM-024], Mignard, F., Tanga, P., 2006, *Window strategies for moving objects*, GAIA-CH-TN-OCA-FM-024, URL http://www.rssd.esa.int/llink/livelink/open/1209978

[FM-047], Mignard, F., Tanga, P., 2011, *The EPSL and the solar system objects*, GAIA-C4-TN-OCA-FM-047, URL http://www.rssd.esa.int/llink/livelink/open/3066195

[PT-002], Tanga, P., 2006, *Identification of Solar System objects with Variable brightness*, GAIA-C7-TN-OCA-PT-002, URL http://www.rssd.esa.int/llink/livelink/open/2705298

M. Connors, P. Wiegert and C. Veillet, 2011. Earths Trojan asteroid, Nature 475, 481-483.

F. Mignard, A. Cellino , K. Muinonen , P. Tanga , M. Delbò , A. Dell'Oro , M. Granvik , D. Hestroffer , S. Mouret , W. Thuillot and J. Virtanen, 2008. The Gaia mission: expected applications to asteroid science, Earth, Moon, and Planets, 101, 97-125.

M. Todd, P. Tanga, D. M. Coward and M. G. Zadnik, 2011. An optimal Earth Trojan asteroid search strategy, MNRAS, in press.

1 Introduction

Observations of Solar System objects with Gaia has already been the subject of several technical notes and papers, describing the science perspectives and the peculiarities of the observing pattern. This has been investigated specifically for main belt asteroids (MBA), near Earth asteroids (NEO or NEA), under the nominal conditions or with the particular scanning law to be used during the DPAC initialisation phase. Documentation is available in the following notes: SAG-FM-007, SAG-FM-009, PT-002, FM-024, FM-047 and in a refereed paper Mignard et al. (2007).

It is known that observations of main belt asteroids are possible only at solar elongations strictly between $45°$ to $135°$, the median being at the quadrature. Also these observations tend to cluster around the two extremes. This is rather easily accounted for by using an average orbit of a main belt asteroid, with low inclination to the ecliptic and small eccentricity, and combining this motion with the geometry of the scanning law. The planetary phases at these elongations remain moderate, around $20°$. A main belt object moves relative to the stellar background with a typical velocity of 10 mas/s, amounting to nearly one pixel shift during one CCD crossing, when this velocity is along scan. The displacement of solar system objects on the Gaia focal plane has serious implications on the windowing scheme adopted for Gaia as explained in (FM-024) as well as on the astrometric precision, in particular for the fastest moving objects. The near Earth objects are much less numerous and fainter, but their geocentric apparent motion could be much larger and above 30 mas/s, a valuable feature to qualify the on-board detection of moving objects, but also a source of complication for the data processing.

In this note we focus on a very particular category of solar system objects, namely the elusive Earth Trojans. The Trojans are minor planets that share the orbit of one of the major planets (or of a satellite in few instances), orbiting around the two Lagrangian point of stability, L4 and L5, lying 60 degrees ahead or behind their parent planet. The first Jupiter trojan was discovered by M. Wolf in 1906 near the Lagrangian point preceding Jupiter (L4) and two more were found within one year. Today several thousands are known around both Lagrangian points of Jupiter. Trojans have also been found associated to Neptune and Mars orbit and until very recently none was connected with the Earth orbit. The discovery of the first Earth trojan (2010 TK7) was officially announced on 28 July 2011 (Connors et al. (2011)), few weeks after this exploration of the Gaia capabilities has started, following discussions that took place during the Solar System Science meeting held in Pisa on 4-6 May 2011.

2 Observability with Gaia

In this qualitative discussion, one can neglect the offset of Gaia with respect to the Earth centre and consider the general geometry of the observations from the geocentre. The Earth trojans are scattered around L4 and L5 as illustrated in Fig. 1, with a distribution which can extend over

several tens of degrees in either directions along the orbit. There is also an extension in the third dimension above or below the ecliptic. One sees immediately the implication for Gaia in terms of observational conditions.

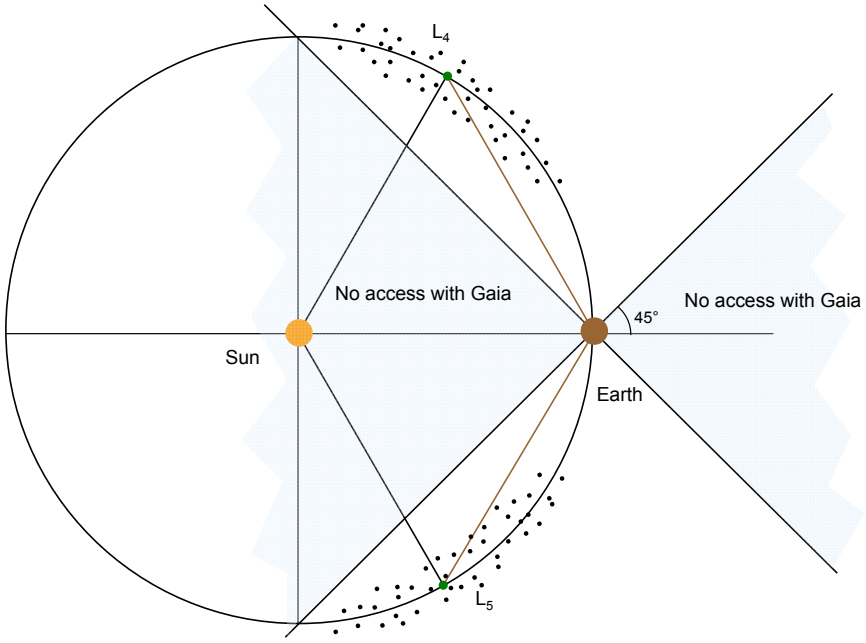


FIGURE 1: Typical distribution of the Earth trojans shown with the observations regions observable with Gaia. They will be seen at small elongation from the sun ($< 90°$) and with a very large phase, above $50°$

.

- The distance to Gaia will of the order of 1 au, ranging between 0.5 to 1.5 au. This is a favorable condition regarding the apparent magnitude. A small body of 1 km in diameter with an albedo of 0.15 has an absolute magnitude $H = 18$. Therefore, neglecting the phase effect (see below) and taking the average situation of an ETA (Earth Trojan Asteroid) at L4-L5 one could, if it were not for the phase, detect planets half that size with Gaia.

- The phase during observations with Gaia will be always large, of the order of $60°$, an unusual feature for the observations of solar system objects. A consequence is a drop of the apparent magnitude by about 1.5 to 2 mag, depending on the surface properties. So at the end, this will limit the detection to planets with diameter of at least 1 km for a planet with an albedo 0.15.

- The solar elongation of L4-L5 is exactly $60°$, and depending on the actual clustering of the planets about the Lagrangian points, a scatter around this number is expected. However, at elongations less than $45°$, there will be no observations with Gaia. Since there will be none, or very few, ETAs with elongation above $90°$, the

elongations during observations of ETAs with Gaia will show a very different distribution as for the main belt asteroids. Indeed, sighting minor bodies at low solar elongation, is a feature which makes their observations from the Earth particularly difficult, while the Gaia capabilities are not altered.

- The typical angular displacement on the sky will be comparable to that of the Sun as seen from the Earth of 1 deg/day, or equivalently 40 mas/s. This is much larger than for a standard asteroid of the main belt by about a factor 3. The projected displacement on the along-scan direction will be on the average smaller, but will remain significantly larger than for a main-belt object. But even at 20 mas/s, this remains large with a blurring of about 1 pixel during a CCD crossing. A slight degradation of the astrometric precision must be considered anyway, that will become quickly much larger with higher transit velocity.

3 Simulation

The general solar system simulation has been run on a series of planets, defined by orbital elements representative of the expected population of Earth-Trojans. Two sets of elements, each for 100,000 objects, have been generated and used as input to the simulator. The first set is composed of circular orbits of 1 au in radius, with various inclinations to the ecliptic. The other osculating elements have been so selected to cluster the planets around L4 and L5. We call this distribution the *Uniform Distribution*. The second set has a random drawing of both the semi-major axis and the eccentricity with $0.9 < a < 1.2$ au and $e < 0.2$. The orbits are then more scattered around the Lagrangian points, with a larger excursion inside and outside the ecliptic. This is referred to as the *Scattered Distribution*. The distribution at a particular epoch (equinox 2012) is shown in projection to the ecliptic in Fig. 2, for both distributions, with red and green dots respectively for the uniform and scattered distributions. The distribution inside the Earth orbit is primarily a projection effect, due to the inclination. In particular all the red dots are in fact at 1 au from the Sun in 3D. An alternative 3D rendering connected to the telescope search strategy is given in Todd et al. (2011).

4 Results of the simulation

Results are presented below in the form of statistical distributions for:

- the solar elongation
- the phase
- the along-scan and cross-scan velocity

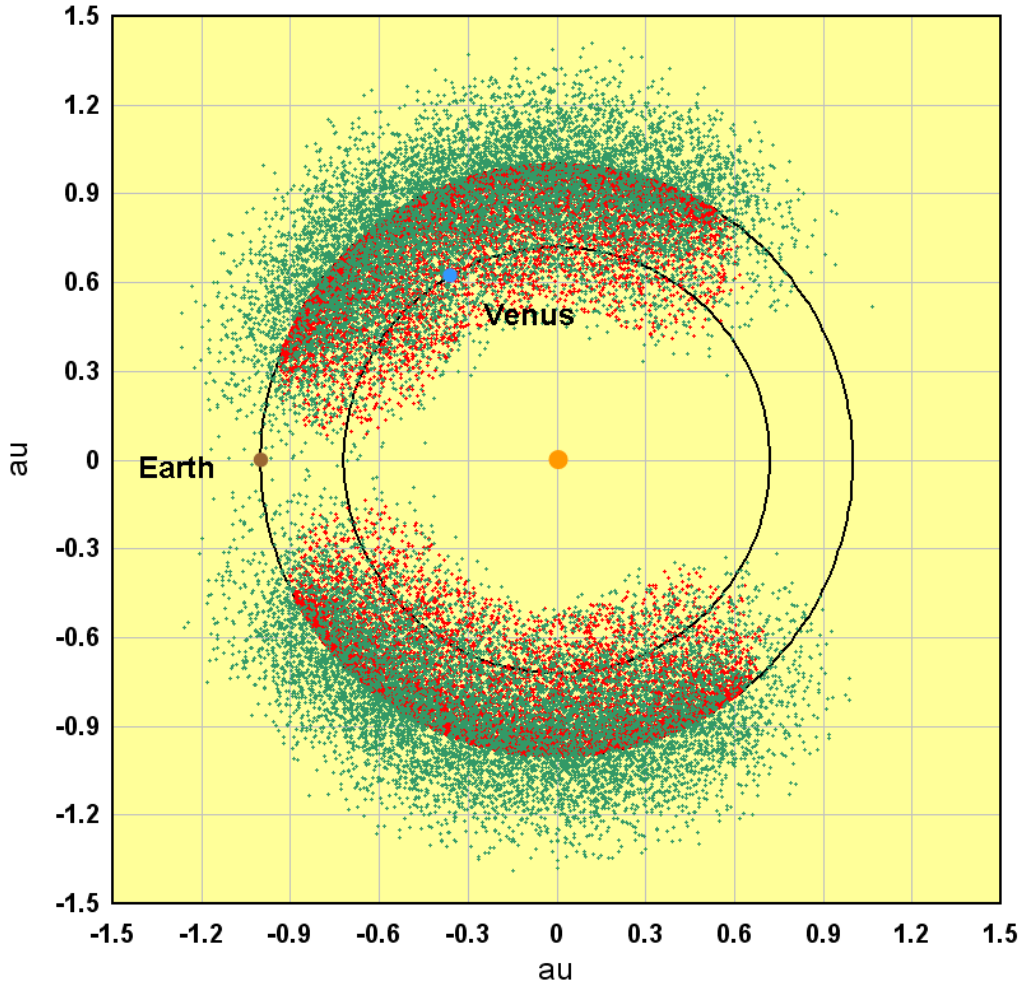


FIGURE 2: Projection on the ecliptic plane of the positions of the simulated Earth Trojans the day of the equinox 2012. The uniform distribution of the orbital elements (all semi-major axes =1) in red dots and the scattered distribution in green. Since the orbits have non-zero inclination, the projection is preferentially inside the ecliptic, an obvious feature for the first set with $a = 1$ au.

- the number of observations

They are presented for the two sets of simulated orbital elements together with the results of a similar simulation run on a similar number of main-belt planets, for the purpose of comparison.

4.1 Solar elongations

Distributions for the solar elongations are displayed in Figs. 3-4 and 5, respectively for the MBAs and the two simulations run on ETAs. The peculiar distribution of elongations for MBAs observed with Gaia has been known since the very first simulations run during the Gaia study phase. The main features is the range of elongations between $45°$ to $135°$ due to the fixed orientation of the scanning plane with respect to the Sun. The second and less intuitive property is the concentration of the observations near the extreme achievable elongations, and the nearly uniform distribution at intermediate elongations, centred one the quadrature. Again, this is well understood from a combination of (i) the precession of the spin axis on a sun-centred cone, and (ii) the fact that most MBAs are observed at very small ecliptic latitude.

Assuming they are all on the ecliptic, these observations can only take place at the nodes between the scanning plane and the ecliptic. Hence, extreme elongations happen at particular phase of the spin-axis precession, namely when this axis lies in the ecliptic. At this point, the line of nodes of the scanning plane with the ecliptic is stationary (Gaia spent more time in the vicinity of this configuration than in the more general ones) and more observations take place during theses phases.

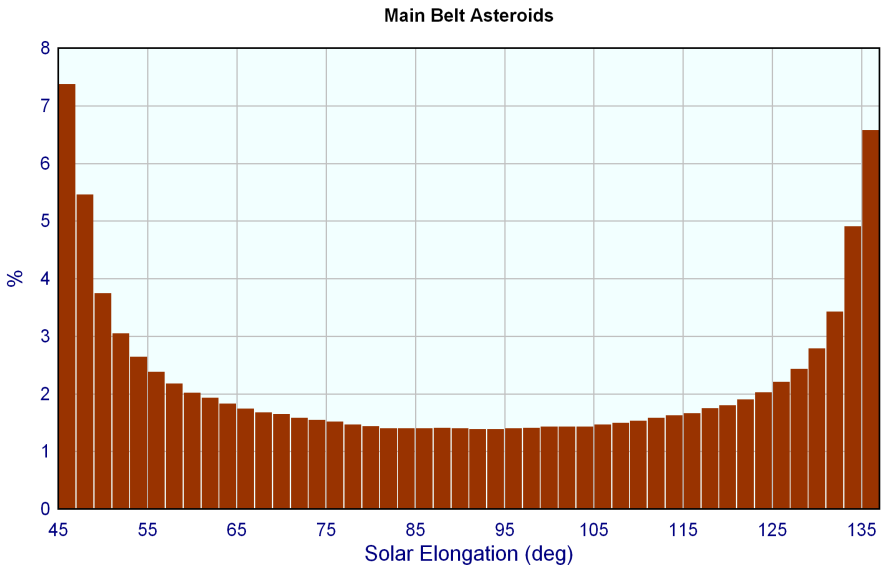


FIGURE 3: Statistical distribution of solar elongations during the observation of the MBA (main-belt asteroids). The main feature of this diagram are perfectly understood and follow from a combination of the geometry of the scanning law and the concentration of asteroids near the ecliptic.

The two plots for the ETAs are, not surprisingly, very different with a limited range of elongations for the reasons explained in Sec. 2. If most of the ETAs were really clustered very close to L4-L5, we would have found a peak in the distribution near $60°$ of elongation, a feature def-

initely not seen. As illustrated in Fig. 2, our simulation reproduces what is actually seen with Jupiter Trojans, with a large scatter around the equilibrium points. Therefore, the effect of the scanning law is predominant and the concentration of elongations remains the largest near $45°$, and decreases slowly to $90°$. In the case of the Scattered Distribution, elongations can be even larger than this limit, due to semi-major axes being larger than 1 au. The drop in the distribution from $45°$ toward larger elongations is less pronounced than with MBA, because of the clustering of ETA around the $60°$ elongations, which compensates a little the pure scanning effect.

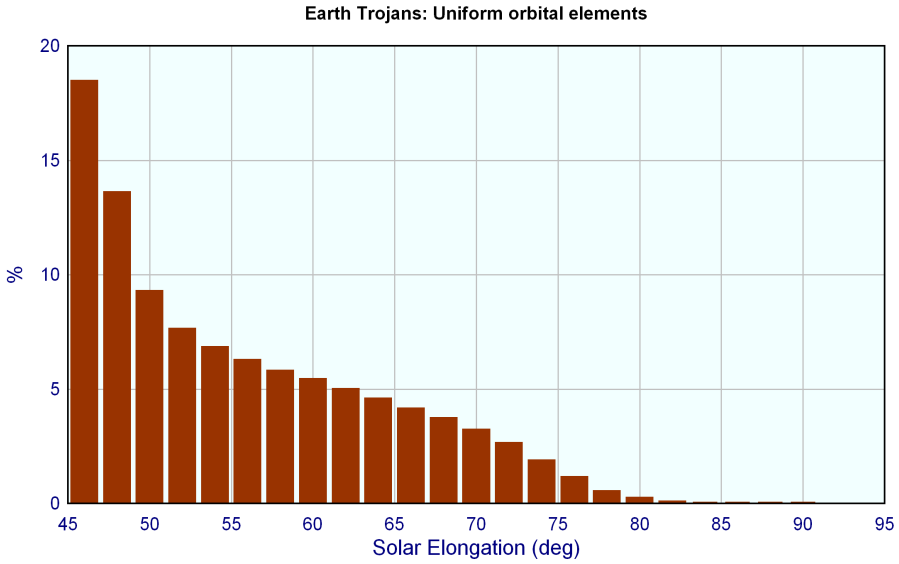


FIGURE 4: Statistical distribution of solar elongations during the observation of the ETAs for the uniform set orbital elements. All objects are observed inside the Earth orbit, and no peak is seen at elongations close to $60°$, since the trojans are in fact well scattered around the Lagrangian points.

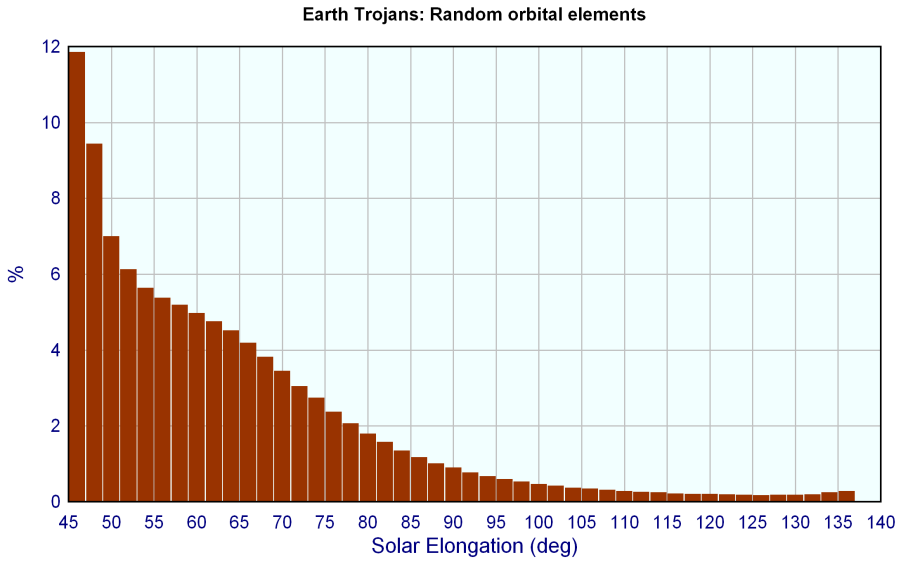


FIGURE 5: Statistical distribution of solar elongations during the observation of the ETAs for the scattered simulated orbital elements. Few planets are outside the Earth orbits and can be observed at elongations larger than 90°.

4.2 Phases

The phases at which a planet is observed is an important issue for the final astrometric accuracy. First, the larger the phase, the less light is collected by Gaia, since a fraction of the surface does not reflect any light. For the same distance to the Sun and to the Earth, the photon related signal-to-noise ratio will be smaller. The second effect comes from the position of the photocentre compared to the centre of mass. The offset is a fraction of the angular diameter and must be allowed for during the orbit fitting, or more generally for any serious astrometric application. The modelling of this effect is far from trivial at the Gaia accuracy level, for object with angular size above few mas. Fortunately the potential ETAs will be all very small, of the order of 1 mas and faint, around the Gaia detection limit. So this correction, even for the very large phases, won't be a serious problem to retrieve the astrometry.

The phase distributions are shown in Figs. 6-7 and 8 respectively for the MBA and the two simulated data sets of ETAs. The difference is striking, with MBAs observed at moderated phases (albeit large for an Earth observer accustomed to taking data near opposition!), while they are very large for ETAs, as expected.

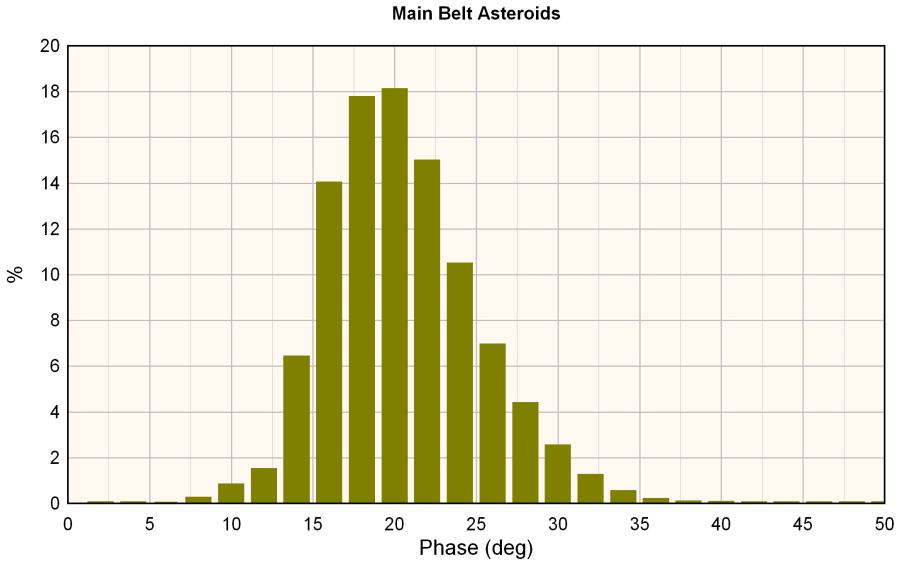


FIGURE 6: Statistical distribution of the phases during the observation of the MBAs with Gaia.

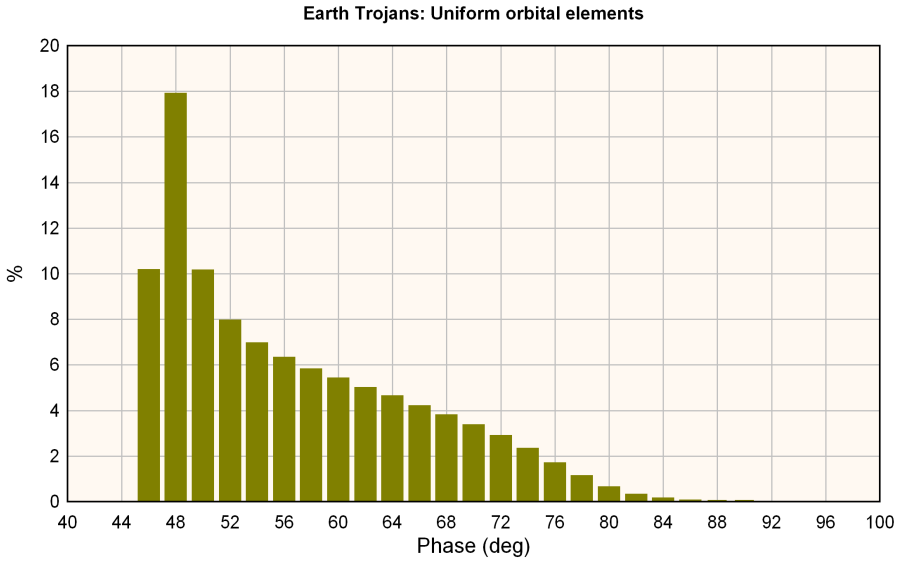


FIGURE 7: Statistical distribution of the phases during the observation of the ETAs for the uniform simulated orbital elements.

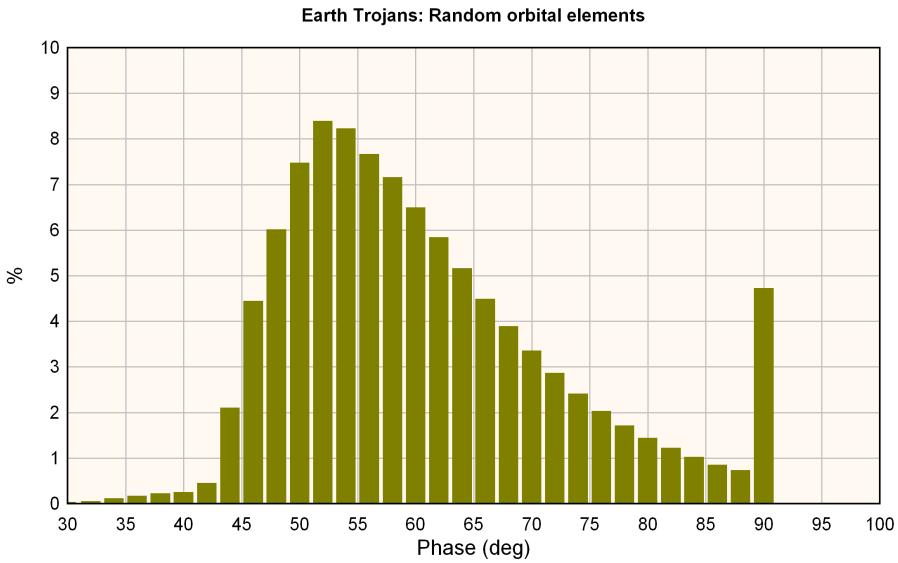


FIGURE 8: Statistical distribution of the phases during the observation of the ETAs for the scattered simulated orbital elements. All phases larger than 90° are counted in the last bin.

4.3 Transit velocity

The velocity of a planet during a transit is a subject of great importance for Gaia, given the size of the field of view and the windowing scheme adopted to track the targets during the field crossing. Objects moving too fast will be lost out of the allocated tracking window before reaching the last CCD column, since the window speed is not adjustable for moving objects. It fits the scan rate perfectly and allows stars to be kept at the centre of the window, from chips to chips. The second issue is the image blurring during the charge transfer from pixel to pixel within a CCD. Again, it is perfectly synchronised to the spin rate and any additional motion of the image will blur the recorded image when the accumulated counts are read out in the serial register. With a pixel of 60 mas, and a crossing time of 4.4 s over one CCD, as soon as the motion of the source relative to the stars reaches 15 mas/s, there is one pixel shift during the crossing, and a loss of astrometric accuracy. With two pixels, or 30 mas/s this loss is quite significant. Simulations by A. Dell'Oro from the Gaia group have shown that the loss in CCD centroiding is about 10% for $V = 20$ mas/s and 50% for $V = 50$ mas/s (A. Dell'Oro, private com.).

Here we have a major difference between MBAs and Earth Trojans. In the first case, the along-scan velocity is generally small enough to avoid significant accuracy loss. One can see in Fig. 9 the distribution of the along-scan velocity for MBAs, which is typically less than 10 mas/s in absolute value. Of course, there are exceptions with the NEAs (Near Earth Asteroids) for which the transit velocity is about three times as large and will be a source of problems in the processing, with unavoidable degradation compared to the nominal accuracy for a star of similar magnitude.

The across-scan velocity distribution is shown in Fig. 10 for the same MBAs, and displays a very characteristic shape, that came initially as a big surprise when these plots were first produced. The two distributions (along- and across-scan) are rather complex in details, and are the compound of three different nearly normal distributions related to the elongations. The features, including the slight asymmetry bump in the along-scan velocity distribution, are all qualitatively well understood and partly explained in FM-047.

For the ETAs, the major difference is the magnitude of the velocity during transit, as shown in Figs. 11 and 12. ETAs with along-scan velocity > 30 mas/s won't be rare, and this will seriously affect the astrometry. Fortunately, during the successive transits of a given object, there will be instances when the velocity is smaller, with no significant loss in astrometric accuracy. A more detailed analysis of the simulation output is required to assess the fraction of perfectly usable transit for each object; this has not been attempted at this stage. The distributions for the uniform and scattered orbital elements are nearly similar, indicating that the results are not very sensitive to the detailed distributions of the orbital elements.

The across-scan velocity distributions are shown in Figs. 13 and 14. One sees again the influence of the geometry with a distribution with small dispersion around ± 40 mas/s. With transverse

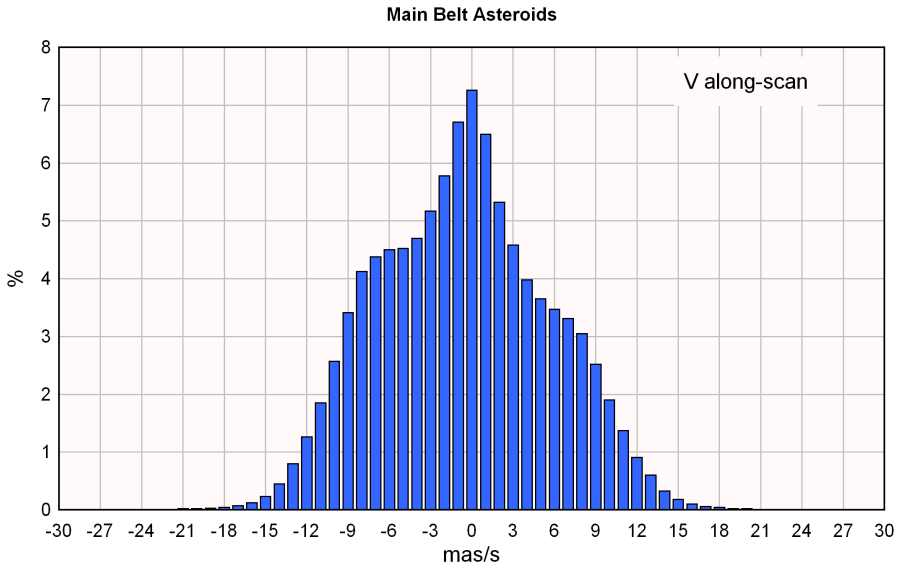


FIGURE 9: Statistical distribution of the along-scan velocity during the observation of the MBAs. For the vast majority of the sources, this transit velocity is not a source of concern for the processing.

velocity of that magnitude, there will be no photometric measurement in the BP/RP CCDs, and even in the astrometric field some CCDs measurement will be lost near the edge of the field since the image will be outside the allocated window. But the detection in the first CCDs columns at the start of the field of view will be sufficient to detect the source, measure its velocity and provide basic astrometry. At this stage this won't be sufficient to tell an ETA from an NEA, but after few transits at different epochs, this should be feasible from a preliminary orbit. Also one may investigate other indicators, like possible correlations between velocity components and elongations and/or ecliptic latitude, that might help discriminate between the two categories in a simpler and probabilistic way.

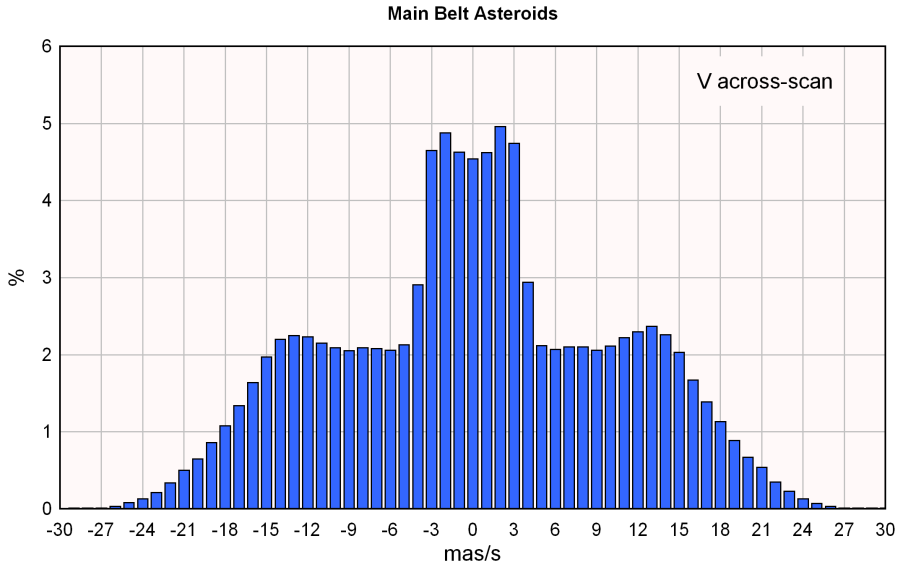


FIGURE 10: Statistical distribution of the across-scan velocity during the observation of the MBAs. For the largest velocities, a problem would arise in the photometric CCDs, as the planet would have slipped outside the tracking window. Correcting measures will be applied on-board.

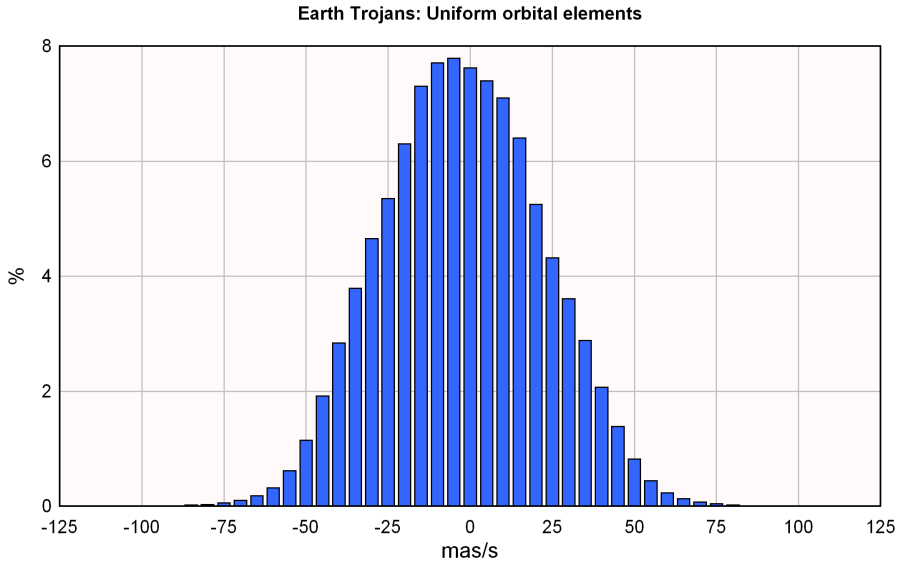


FIGURE 11: Statistical distribution of then along-scan velocity during the observation of the ETAs for the uniform simulated orbital elements.

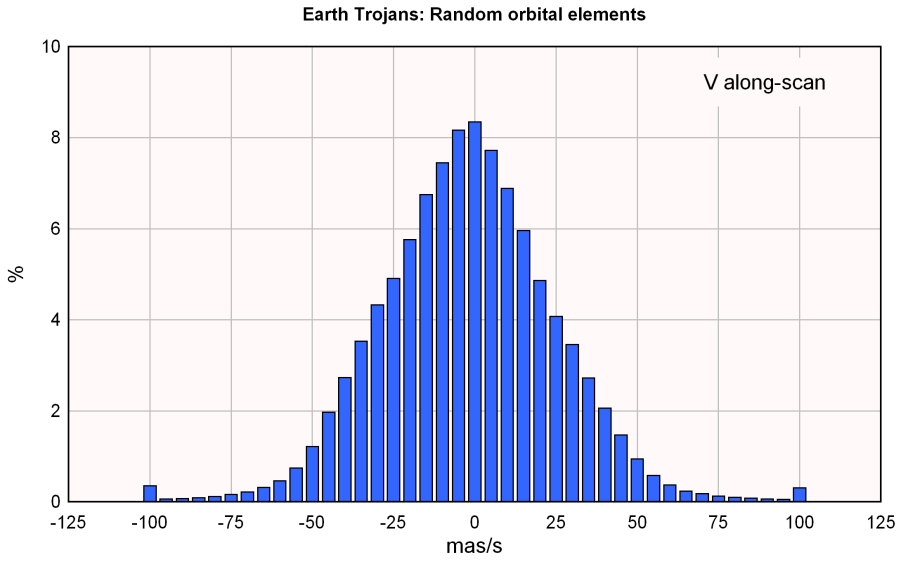


FIGURE 12: Statistical distribution of the along-scan velocity during the observation of the ETAs for the scattered simulated orbital elements.

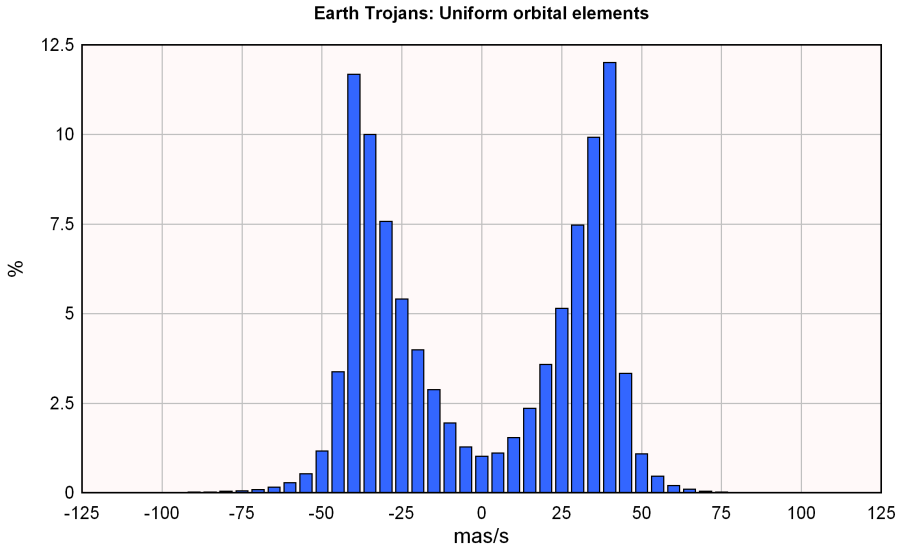


FIGURE 13: Statistical distribution of the across-scan velocity during the observation of the ETAs for the uniform simulated orbital elements.

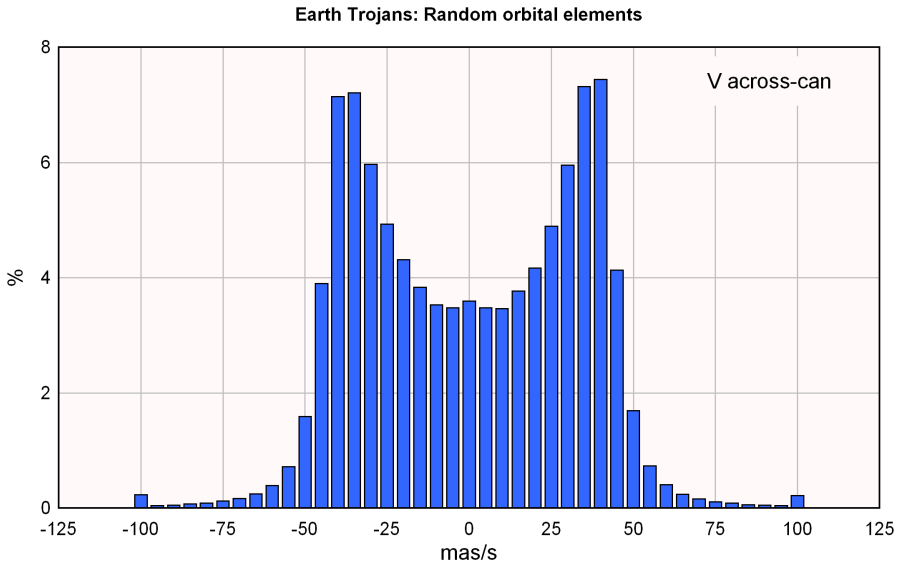


FIGURE 14: Statistical distribution of the across-scan velocity during the observation of the ETAs for the scattered simulated orbital elements.

4.4 Number of transits

The last set of plots concerns the number of observations during the 5-year Gaia nominal mission. Here one observation is equivalent to one field crossing which in fact produces normally 9 independent CCDs measurements, over a timespan of 40s. The sky average for the stars is about 85 transits (neglecting dead-time), with a well defined variation as a function of the ecliptic latitude. Sources of low ecliptic latitude (in absolute value) are under-observed, while at $b = 45°$, there is a significantly higher number of observations. Main-belt asteroids being always close to the ecliptic, the average number is of the order of 65, as seen in Fig. 15. The scatter about the mean is quite large, and by pure chance effect (in fact this is a fully deterministic situation once the scanning law parameters are fixed), some planets are observed more often than others, and possibly with extended continuous sequences over several spin periods. However the standard case is a pair of crossings in the preceding and following field, and an interval of few weeks before a new pair of observations is achieved. The fact that there are sources with a very small number of observations results also from the planets having during some transits a magnitude > 20, thus not detected by Gaia. This feature is taken care of in the simulation. Main belt objects with $H > 16-17$, have all several passages in the fields of view with too faint a magnitude to be seen by Gaia.

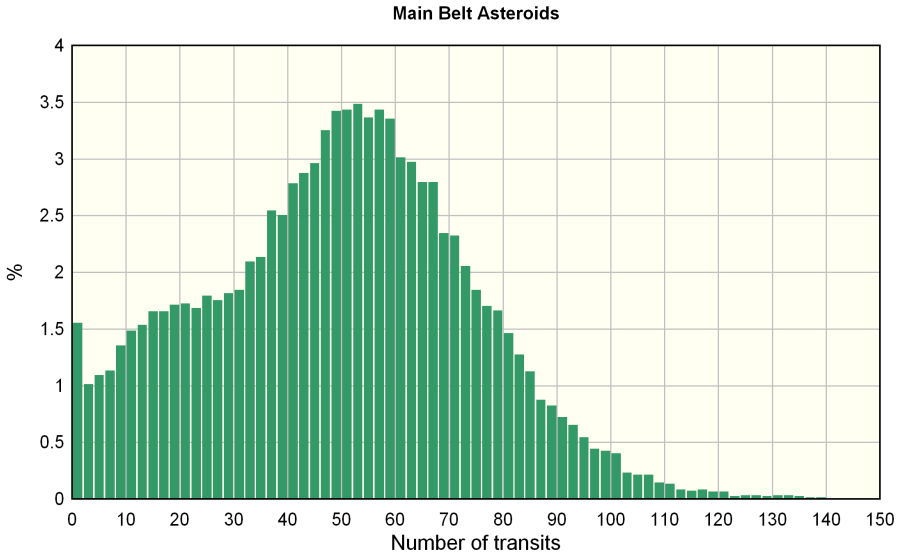


FIGURE 15: Statistical distribution of the number of detected transits ($G < 20$) during the observations of the MBAs. The average is about 65, with an extended tail up to 100 transits. The large number of under-observed sources (compared to stars) results from the variable magnitude of MBAs at crossing times, smaller objects being sometimes fainter than Gaia detection limit.

Similar plots are drawn for the ETAs and shown in Figs. 16 and 17. In the simulation the object have an absolute magnitude $H = 17.35$ and The difference between the apparent magnitude and the absolute magnitude is much smaller than for the MBAs because of the distance: typically 1 au from the Sun and from the Earth. However the phase is larger, and there is a drop of about

2 magnitude, meaning that most of the ETAs in this simulation are detected at an apparent magnitude of $\sim 19 - 19.5$. The few which are not detected appear in the distributions in the first bin, with no observation at all. Otherwise the difference between the uniform and scattered distributions comes from the phases, which are larger for the second distribution (Figs. 7-8) leading to a fainter apparent magnitude, probably just above 20.

But another reason for the large number of never observed planets, and not shared by MBAs, comes from the elongations. Some of the simulated orbits may produce objects which always lie within less than $45°$ from the Sun, and not accessible to Gaia. This is a reasonable guess from Fig. 2, although the 2D projection may be misleading.

It is useful to recall that the motions of the planets are not numerically integrated (2-body propagation instead) with the Jupiter perturbation. This option is available in one version of the simulation program, but has not been activated in this work which aims for global statistical results, for which a Keplerian motion is sufficient, and faster to run.

The main point to emphasize here is the fact that on the average ETAs, geometrically and photometrically accessible to Gaia, are over-observed compared to MBAs. This increases the odds in favour of their detection and also offers the opportunity to get a better astrometric solution, compared to an MBA of comparable magnitude.

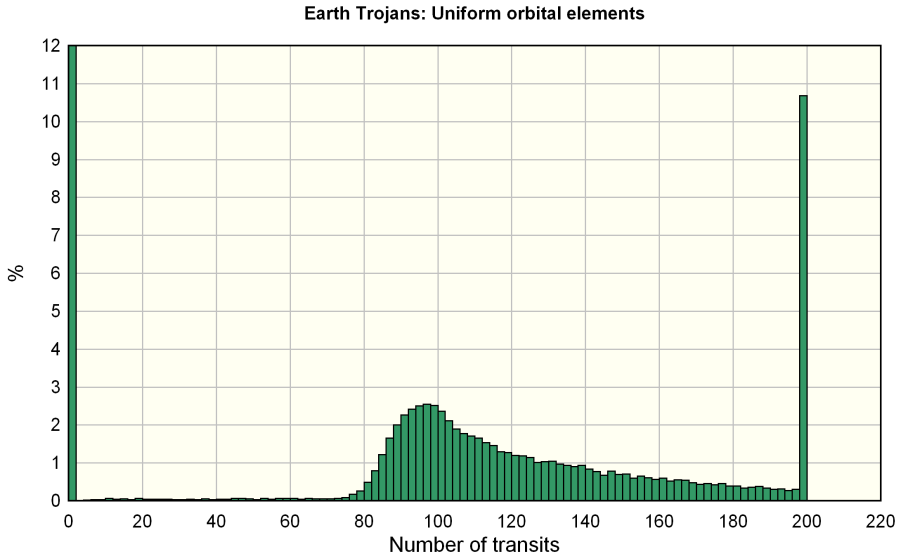


FIGURE 16: Statistical distribution of the number of detected transits ($G < 20$) during the observations of the ETAs for the uniform simulated orbital elements. All sources with more than 200 observations are counted in the last bin. The first bin, with no observation at all accounts for 22% of the simulated planets, because of their elongation being too small.

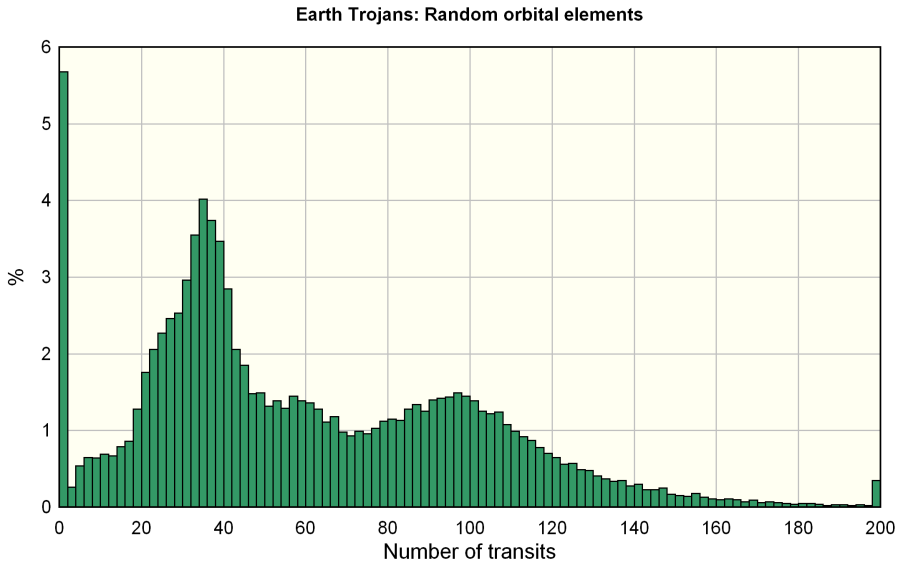


FIGURE 17: Statistical distribution of the number of detected transits ($G < 20$) during the observations of the ETAs for the scattered simulated orbital elements. All sources with more than 200 observations are counted in the last bin.

5 Conclusions

Using realistic orbital elements of potential Earth Trojan asteroids we have simulated their observations with Gaia over the missions expected length of 5 years. Results have been produced by comparing the condition of detection and the properties of the measurements to a similar simulation for a set of comparable size of main belt asteroids. The main results obtained are:

- Provided the libration orbit allows an ETA to enter the field of view of Gaia, these planets are, on the average, observed on more transits than a standard main belt object. The increase is at least 50%, depending on the orbit and magnitude.
- The along-scan transit velocity is much larger than for a standard MBA, leading to a significant image blurring and consequently a loss in astrometric accuracy. How big it is has not yet been quantified.
- The drop between the absolute magnitude and the apparent magnitude at crossing time is much smaller for ETAs (they are closer to the Earth) than for the MBAs. This means that object with diameter of 1km, or slightly below, could be detected.
- The phases during the crossings of an ETA are statistically much larger than for a main belt planet. This make them fainter for identical distances and size. However, given the small size expected, and the astrometric degradation due to image blurring, dealing with the photocentre offset will not present a great problem.